In Vivo Interactome of *Helicobacter pylori* Urease Revealed by Tandem Affinity Purification*

Kerstin Stingl‡§¶, Kristine Schauer‡‖, Chantal Ecobichon‡ ‡‡, Agnès Labigne‡, Pascal Lenormand§§, Jean-Claude Rousselle§§, Abdelkader Namane§§, and Hilde de Reuse‡‖¶¶**

In the human gastric bacterium *Helicobacter pylori*, two metalloenzymes, hydrogenase and urease, are essential for *in vivo* colonization, the latter being a major virulence factor. The UreA and UreB structural subunits of urease and UreG, one of the accessory proteins for Ni^{2+} incorporation into apourease, were taken as baits for tandem affinity purification. The method allows the purification of protein complexes under native conditions and physiological expression levels of the bait protein. Furthermore the tandem affinity purification technology was combined with *in vivo* cross-link to capture transient interactions. The results revealed different populations of urease complexes: (i) urease captured during activation by Ni^{2+} ions comprising all the accessory proteins and (ii) urease in association with metabolic proteins involved *e.g.* in ammonium incorporation and the cytoskeleton. Using UreG as a bait protein, we copurified HypB, the accessory protein for Ni^{2+} incorporation into hydrogenase, that is reported to play a role in urease activation. The interactome of HypB partially overlapped with that of urease and revealed interactions with SlyD, which is known to be involved in hydrogenase maturation as well as with proteins implicated in the formation of [Fe-S] clusters present in the small subunit of hydrogenase. In conclusion, this study provides new insight into coupling of ammonium production and assimilation in the gastric pathogen and the intimate link between urease and hydrogenase maturation. *Molecular & Cellular Proteomics 7: 2429–2441, 2008.*

Protein-protein interactions are operative at the majority of cellular processes; thus, their study gives valuable insight into proteomic and functional associations. *Helicobacter pylori* is a Gram-negative bacterium that is infecting the stomach of about half of the human population. It is responsible for the development of gastric pathologies such as gastritis, gastroduodenal ulcer, and adenocarcinoma (1). One remarkable feature of *H. pylori* is its capacity to persist (often during decades) and multiply in the hostile environment of the stomach. In *H. pylori*, urease is a major virulence factor and is essential for the resistance to acidity because of its capacity to hydrolyze urea into bicarbonate and ammonia (2), which results in pH homeostasis of the bacterium. The protein is an extremely active and highly regulated member of the nickel metalloenzyme family. Activation of urease, *i.e.* incorporation of nickel into the active site, requires urease-specific accessory proteins whose homologues have been extensively studied genetically and biochemically in *Klebsiella pneumoniae* (3–8). It is still enigmatic why vast amounts of urease, up to 10% of the total protein, are produced, whereas only a minor active portion is sufficient for acid resistance (9). Furthermore the observation that urease is even indispensable for the colonization under neutral conditions (10) suggested additional essential functions for this central enzyme that remained unidentified.

H. pylori possesses another nickel-containing enzyme, a [NiFe] hydrogenase, allowing this organism to utilize hydrogen as an energy source. Accordingly hydrogenase has been shown to be essential for *H. pylori* colonization in the mouse model (11). The assembly of the [NiFe] hydrogenase metal center located in the large hydrogenase subunit is partially understood and requires several proteins involved in the sequential delivery of iron before nickel (for a review, see Ref. 12). In addition, the [NiFe] hydrogenase possesses a small subunit containing [Fe-S] clusters. For the assembly of the latter no distinct biosynthetic pathway has been attributed so far, suggesting that the housekeeping [Fe-S] cluster assembly system might be involved (12). *H. pylori* is unique in that the maturation events of these two nickel-containing essential proteins are interconnected as *H. pylori* mutants deficient in one of the accessory proteins, HypA or HypB, involved in nickel insertion into hydrogenase, lack significant activation of urease (13).

From the ‡Unité de Pathogénie Bactérienne des Muqueuses, ‖Unité Postulante de Pathogenèse de *Helicobacter*, ‡‡G5 Biologie et Génétique de la Paroi Bacterienne, and §§Plate-forme de Protéomique, Institut Pasteur, 75015 Paris, France and §Institut für Allgemeine Zoologie und Genetik, Westfälische Wilhelms-Universität, 48149 Münster, Germany

Received, April 11, 2008, and in revised form, June 24, 2008

Published, MCP Papers in Press, August 4, 2008, DOI 10.1074/mcp.M800160-MCP200

The yeast two-hybrid (Y2H)[1] analysis, which tests for binary protein complexes, has been applied in large scale proteome analysis of yeast and other eukaryotes (14, 15) and was also applied in *H. pylori* (16). However, the Y2H data are hampered by protein overexpression and by the use of a heterologous system for analysis, resulting in a relatively high false positive *versus* true positive ratio. Recently a protein interaction study based on the co-migration of proteins in a complex visualized by blue native/SDS-PAGE separation was performed in *H. pylori*, leading to results that are difficult to interpret because of the naturally limited protein resolution in this system (17). An alternative method, namely the tandem affinity purification (TAP) technique, has proven to be an efficient means to access multipartner protein complexes with fewer false positives and much better function predictions than from Y2H data (18–20). This method implies the expression of a bait protein fused to two different tags in tandem (protein A of *Staphylococcus aureus* and the calmodulin binding domain) at physiological levels in the organism of origin. The bait protein in complex with its interaction partners is purified under native conditions, therefore maintaining complex integrity. Purification by two successive affinity chromatography steps guarantees an outstanding specificity. Subsequently the copurified proteins are separated on a gel and individually identified by mass spectrometry. This technique has been applied to a variety of eukaryotic systems from yeast to human cells (21–23) but is, surprisingly, still restricted to the model prokaryote *Escherichia coli* with a small number of reported studies (24–28).

The present work represents the first application of TAP to the study of a bacterial pathogen. We intended to highlight the interactome of urease and associated proteins. In addition, we established a new strategy to capture transient protein complexes by *in vivo* cross-link prior to TAP. This procedure was proven to be powerful and complementary to the classical TAP strategy as our results both confirmed expected data and revealed new links between urease and ammonium assimilation as well as with components of the cytoskeleton. Furthermore we found an *in vivo* interaction between the nickel maturation systems for urease and hydrogenase that provides an extended view on the previously observed functional relationship between the two.

EXPERIMENTAL PROCEDURES

Strains and Growth Conditions

H. pylori strain 26695 was grown either on blood agar plates (Oxoid) supplemented with 10% defibrillated horse blood (bioMérieux) or in liquid culture using brain-heart infusion (Oxoid) with 3% fetal bovine serum (Invitrogen). Antibiotics were used at the following final concentrations: 12.5 μg/ml vancomycin, 3.1 μg/ml polymyxin B, 6.25 μg/ml trimethoprim, and 2.5 μg/ml amphotericin B. For the TAP-tagged mutants, kanamycin was added at 20 μg/ml. Plates were incubated at 37 °C under a microaerobic atmosphere in an anaerobic jar using a carbon dioxide-generating and oxygen-consuming system (CampyGen, Oxoid). Liquid cultures were shaken at 140 rpm.

E. coli strain MC1061 (29) was grown at 37 °C in Luria broth (30) with 100 μg/ml ampicillin or carbenicillin, 100 μg/ml spectinomycin, or 20 μg/ml kanamycin if appropriate. Transformation of *H. pylori* was carried out as described previously (31). Cells that had recombined the tag into the chromosome were selected by their resistance to kanamycin.

Construction of pILL851C Carrying the C-terminal TAP Tag Fused to a Non-polar Kanamycin Resistance Cassette

The non-polar kanamycin resistance cassette was amplified from pUC18ΔK2 (32) using the forward primer H152 (supplemental Table S1) containing a BglII site and the reverse primer H153 (supplemental Table S1) containing a HindIII site. The resulting PCR product was cut by BglII and HindIII and ligated into pILL570Not (33) opened by the same restriction enzymes, leading to the plasmid pILL570Not-Kana. The C-terminal TAP tag was amplified from pBS1479 (18) using the forward primer H150 (supplemental Table S1) and the reverse primer H151 (supplemental Table S1) both containing BamHI as restriction site. The amplified product was cut by BamHI and ligated into pILL570Not-Kana opened with BglII and BamHI. The direction of the insertion of the C-terminal TAP tag was verified by restriction and later sequenced. The plasmid carrying the C-terminal TAP tag fused in front of the non-polar kanamycin cassette was named pILL851C (see Fig. 1).

Construction of C-terminal TAP Fusion Genes on the Chromosome of H. pylori 26695

For the construction of genes fused to the C-terminal TAP tag (illustrated in Fig. 1), around 500 base pairs of the 5′- and the 3′-regions flanking the TAP insertion site, *i.e.* the stop codon of the target gene, were amplified using genomic DNA of *H. pylori* 26695. For the 5′-region, a gene-specific forward primer containing a restriction site for PstI and 25 homologous nucleotides upstream of the TAP insertion site (A2) was used with a reverse primer containing 21 homologous nucleotides immediately upstream of the insertion site in frame with the tag-specific priming regions at the start of the C-terminal tag (5′-CTCTTTTCCATGGATCC-3′) (A1). For amplification of the 3′-region flanking of the TAP insertion site, a forward primer containing the tag-specific priming regions at the 3′-end of the C-terminal tag (5′-TAGTACCTGGAGGGAATA-3′) and 21 homologous nucleotides immediately downstream of the insertion site (B1) was used with a gene-specific reverse primer containing 25 homologous nucleotides downstream of the TAP insertion site and a restriction site for ClaI (B2). Moreover the C-terminal TAP tag was cut out of pILL851C using PstI and ClaI. The two PCR products and the restriction product were purified over an agarose gel using Qiaquick columns (Qiagen) before mixing 50 ng of the C-terminal TAP tag with equimolar amounts of the two flanking regions (A1-A2 and B1-B2). The complete fragment containing the C-terminal TAP tag flanked by the two gene-specific regions, A1-A2 and B1-B2, was amplified using the primer pair A2, B2. After purification over an agarose gel the fragment was cut with PstI and ClaI and cloned into pILL570Not opened with the same restriction enzymes. The plasmid harboring the C-terminal tag fused to the flanking regions of the stop codon of the target gene was transformed to *E. coli* MC1061 and purified using the Midiprep kit (Qiagen). After transformation of 10–20 μl of the plasmid to *H. pylori* 26695, cells that had recombined the tag into the chro-

[1] The abbreviations used are: Y2H, yeast two-hybrid; TAP, tandem affinity purification; DSP, dithiobis(succinimidyl) propionate; TEV, tobacco etch virus; GlnA, glutamine synthetase; STRING, search tool for the retrieval of interacting genes/proteins.

mosome were selected by their resistance to kanamycin and were checked for expression of a tagged fusion protein by Western blot.

Purification of TAP-tagged Proteins from H. pylori

H. pylori cells of late logarithmic phase (2 liters of OD = 0.7–1) were harvested, washed once with 1% KCl, and stored at −80 °C. The purification procedure was performed in principle according to the method of Rigaut *et al.* (18) with some modifications in the buffer compositions. Thus, cells were suspended in 10 ml/g lysis buffer (100 mM HEPES/KOH, pH 7.4, 100 mM KCl, 8% glycerol, Complete protease inhibitor (Roche Applied Science)) and either sonicated three times for 2 min at 2.5 output, 50% pulsed (Branson sonifier model 450) or disrupted by French press. After centrifugation of cell debris (33,000 × *g* for 30 min), 0.1% Nonidet P-40 was added before binding of the protein extract to 0.2 ml of Sepharose-IgG beads (Amersham Biosciences) for 2 h at 4 °C. The beads were recovered by low speed centrifugation, pipetted to a flow-through column, and washed with 10 ml of binding buffer (50 mM HEPES/KOH, pH 7.4, 100 mM KCl, 0.1% Nonidet P-40, Complete protease inhibitor (Roche Applied Science)) supplemented with 0.5 mM DTT. To release the IgG-bound complex, 250 μl of binding buffer with 0.5 mM DTT and 10 units of AcTEV protease (Invitrogen) were added to the beads and incubated at 16 °C for 2 h. The eluate was added to the same volume of binding buffer supplemented with 4 mM $CaCl_2$ and incubated with 75 μl of calmodulin beads (Stratagene) at 4 °C for 1 h. The beads were washed with 5 ml of binding buffer supplemented with 2 mM $CaCl_2$, and the protein complex was eluted with 400 μl of 20 mM Tris/HCl, pH 8, 50 mM NaCl, 5 mM EGTA. Proteins were precipitated with 10% TCA, washed once with 95% ethanol, and solubilized in Lämmli loading buffer with 50 mM DTT as reducing agent for 20 min at 80 °C. Proteins were separated on a 5–20% gradient Lämmli SDS-polyacrylamide gel and stained with colloidal Coomassie (34). Protein bands were cut out, digested with trypsin, and analyzed by mass spectrometry.

Cross-linking of Protein Complexes and Modifications of the Purification Method

Cells were suspended in lysis buffer as described before. The thiol-cleavable cross-linker dithiobis(succinimidyl propionate) (DSP) was added at a concentration of 200 μg/ml and incubated for 5 min on ice. The cross-link reaction was stopped by the addition of 10 mM Tris/HCl, pH 7.4. The purification proceeded as for non-cross-linked samples except that the protein complex was eluted from the IgG-Sepharose twice with 400 μl of 100 mM glycine-HCl, pH 3, supplemented with 100 mM KCl. The eluate was mixed with 800 μl of binding buffer supplemented with 4 mM $CaCl_2$, and the pH was readjusted to 7 by addition of KOH before binding to the calmodulin beads. The purification was continued as for non-cross-linked samples.

Western Blot Analysis

The proteins in fusion with the TAP tag were detected by Western blot analysis using a peroxidase-coupled anti-peroxidase antibody (Sigma).

Identification of Proteins by Mass Spectrometry

Sample Preparation—After Coomassie staining all visible gel bands were excised using the robotic work station ProPic Investigator (Genomic Solutions, Ann Arbor, MI), and plugs were collected in a 96-well plate. Destaining, reduction, alkylation, and trypsin digestion of the proteins followed by peptide extraction were carried out with the ProGest Investigator (Genomic Solutions). After desalting (C_{18}-μZipTip, Millipore) peptides were eluted directly using the ProMS Investigator (Genomic Solutions) onto a 96-well stainless steel MALDI target plate (Applied Biosystems/MDS SCIEX, Framingham, MA) with 0.5 μl of α-cyano-4-hydroxycinnamic acid matrix (2.5 mg/ml in 70% acetonitrile, 30% H_2O, 0.1% trifluoroacetic acid).

Mass Spectrometry Analysis—Raw data for protein identification were obtained on the 4800 Proteomics Analyzer (Applied Biosystems, Framingham, MA) and analyzed by GPS Explorer 2.0 software version 3.6 (Applied Biosystems). For positive ion reflector mode spectra 3000 laser shots were averaged. For MS calibration, autolysis peaks of trypsin ($[M + H]^+ = 842.5100$ and 2211.1046) were used as internal calibrators. Monoisotopic peak masses were automatically determined within the mass range 800–4000 Da with a signal to noise ratio minimum set to 30. Up to 12 of the most intense ion signals were selected as precursors for MS/MS acquisition excluding common trypsin autolysis peaks and matrix ion signals. In MS/MS positive ion mode, 4000 spectra were averaged, collision energy was 2 kV, collision gas was air, and default calibration was set using Glu^1-fibrinopeptide B ($[M + H]^+ = 1570.6696$) spotted onto 14 positions of the MALDI target. Combined peptide mass fingerprint and MS/MS queries were performed using the MASCOT search engine 2.1 (Matrix Science Ltd., London, UK) embedded into GPS Explorer software on the *H. pylori* database (PyloriGene, data release R1.6, 1654 entries) (35) with the following parameter settings: 50-ppm mass accuracy, trypsin cleavage with one missed cleavage allowed, carbamidomethylation set as fixed modification, oxidation of methionines allowed as variable modification, and MS/MS fragment tolerance set to 0.3 Da. Protein hits with MASCOT protein score ≥45 and a GPS Explorer protein confidence index ≥95% were used for further manual validation.

RESULTS AND DISCUSSION

Genetic Tools and Expression of TAP Fusion Proteins in H. pylori—To adapt the TAP method to study protein complexes in *H. pylori*, we constructed plasmid pILL851C, which contained an insert with two consecutive modules: (i) the sequences necessary for C-terminal TAP tagging of a target or bait protein (composed of the sequence of protein A, a TEV protease cleavage site, and the calmodulin binding domain) followed by (ii) a non-polar kanamycin resistance cassette as a selection marker in *H. pylori* (36) (Fig. 1). As illustrated in Fig. 1, this plasmid served as a template for a rapid PCR-based fusion with the flanking regions of any target gene that we wanted to tag in its original genetic locus on the chromosome of *H. pylori*.

The TAP-tagged proteins and their interacting partners were purified via two successive affinity columns (Fig. 2), and the interactors were identified by mass spectrometry after migration on an SDS-polyacrylamide gel. Therefore, the use of a strain whose genome was entirely sequenced such as strain 26695 (37) was mandatory. Direct natural transformation of the PCR product carrying the fused TAP tag gene plus 500 bp of the respective regions flanking the insertion site led to no or sporadic transformants in the *H. pylori* strain 26695. The efficiency of transformation was significantly increased by an additional cloning step of the PCR product into a plasmid that was not able to replicate in *H. pylori*.

The tandem affinity purification method relies on the specific interaction between protein A and IgG during the first affinity chromatography step. Because protein A interacts

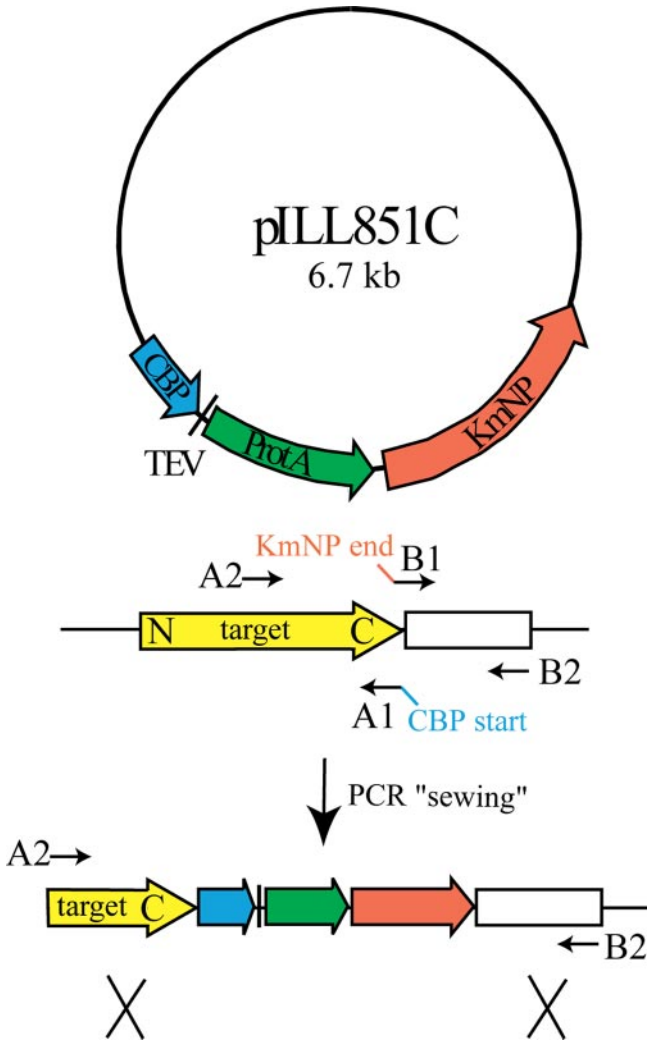

FIG. 1. **Construction of C-terminal TAP fusion genes for recombination into the *H. pylori* chromosome.** Chromosomal regions flanking the insertion site of the TAP tag (*i.e.* directly before the stop codon) were amplified using the primer pairs A1, A2 and B1, B2. The A1 and B1 primers carry additional nucleotides complementary to the 5′-end or the 3′-end of the TAP tag (in pILL851-C), respectively, to enable fusion of the TAP tag with the flanking regions by PCR sewing. Sites at which homologous recombination into the chromosome can occur are indicated by *crosses*. *CBP*, calmodulin-binding protein; *KmNP*, kanamycin non-polar cassette; *TEV*, cleavage site of the TEV protease; *C*, region of the target gene encoding the C terminus of the protein; *N*, region of the target gene encoding the N terminus of the protein; *ProtA*, protein A.

with the conserved region of IgG, any secondary antibody can in principle be used for the detection of TAP-tagged proteins. Eleven genes (Table I) were targeted, and the production of the corresponding fusion proteins was examined by immunoblot with a peroxidase-coupled antibody in crude extracts of the *H. pylori* strains (Fig. 3). Most bait proteins (Table I) were chosen because their function has been associated with ammonia and urea metabolism, which is crucial for *H. pylori* virulence (urease structural and accessory proteins, arginase, and hydrogenase accessory protein) or because they were found to be differentially expressed under acid stress conditions (AmiE, AmiF, HslU, and MetK) (13, 38–40). In addition, DnaQ, an essential protein used in the TAP study of *E. coli*, was added for comparison (24). All fusion proteins were stably expressed in *H. pylori* and detected in a highly sensitive and specific manner (Fig. 3). The use of an alternative sequential peptide affinity tag in which the protein A is replaced by the smaller FLAG epitope was reported for tandem affinity purification in *E. coli* and human cell lines (41). However, the monoclonal antibody (M2) commonly used for detection and purification of FLAG-tagged proteins was not suitable for the study in *H. pylori* because it showed considerable cross-reactivity with *H. pylori* protein extracts (data not shown).

Several proteins that are essential for *in vitro* growth were successfully tagged, showing that the TAP tag did not interfere with their functions. Examples are DnaQ and *S*-adenosylmethionine synthetase (MetK) (Table I and Fig. 3) as well as DnaA (HP1529) and HP1230 not discussed in the present study (42). Glutamine synthetase (GlnA) encoded by *hp0512* was a notable exception. Furthermore we addressed the enzymatic activity of several tagged proteins as a control. Tagging urease we observed a partial loss of activity. For UreA-TAP this amounted to 6-fold, and for UreB-TAP at least 40-fold less activity was measured in cell extracts. In contrast, UreG-TAP was fully functional because urease activity was similar to that in wild-type bacteria, and enhanced Ni^{2+} incorporation into urease at pH 5, measured as in Schauer *et al.* (43), was not affected (data not shown). Subsequently the ability to purify the TAP-tagged protein was tested. Except for DnaQ-TAP, all proteins could be purified, however, with different yields. Purification of DnaQ-TAP failed probably because the tag was not accessible for the affinity columns. AmiE-TAP and AmiF-TAP were only purified in traces (data not shown). Because nearly no proteins were purified with these three bait proteins, we concluded that protein extracts of *H. pylori* do not bind unspecifically to the affinity columns and that copurified proteins inevitably come from interaction with the TAP-tagged protein.

Extending the TAP Method to Purification of Transient Interactions by in Vivo Cross-link—Purification via two independent affinity columns requires stable complexes that survive the whole purification process. Likewise the genome-wide protein interaction study of *E. coli* was mostly exemplified by stable protein complexes like DNA and RNA polymerases and acyl-carrier protein complex for fatty acid biosynthesis (24, 26). Using the classical TAP method, there is a high probability to loose transient interactions, which probably represent the majority of all cellular interactions. To capture transient interactions in the whole cell context and subsequently break the cells to purify the TAP-tagged protein and its protein partners, we developed a novel strategy starting with an *in vivo* cross-link of whole *H. pylori* cells. An analogous approach was successfully applied for pulldown experiments

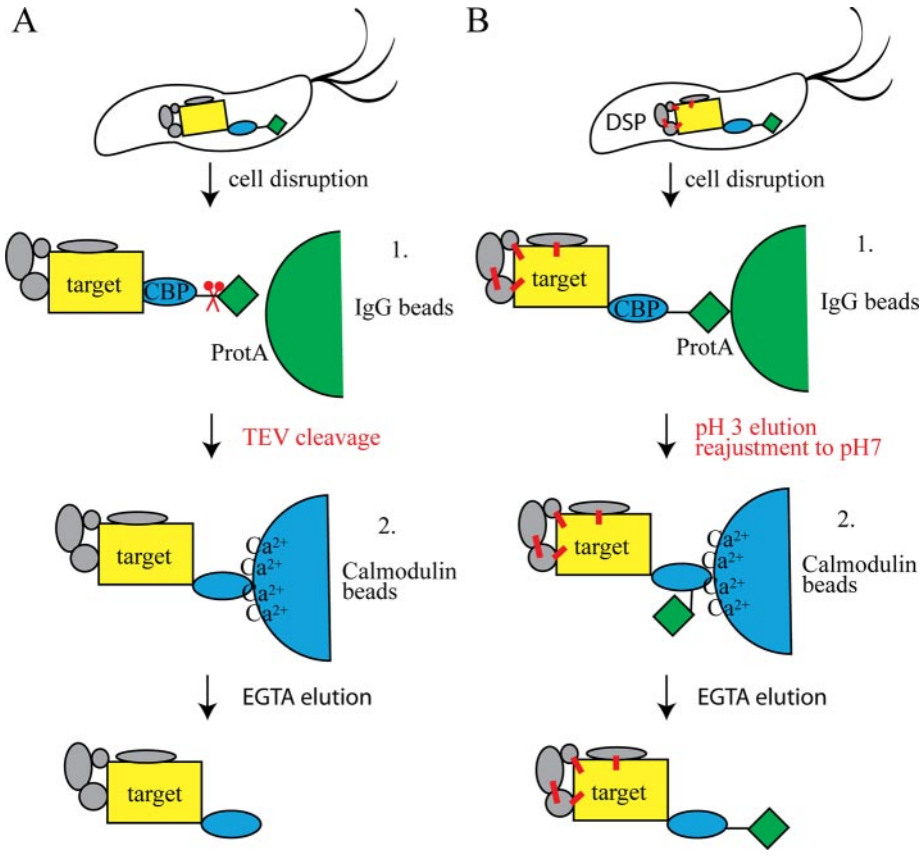

FIG. 2. **Principle of the TAP method modified (according to Rigaut *et al.* (18).** *A*, purification under native conditions; *B*, purification after cross-link of protein complexes in whole cells using DSP. Both purification methods were performed in parallel for each TAP-tagged protein and resulted in overlapping and complementary results. *CBP*, calmodulin-binding protein; *ProtA*, protein A.

TABLE I
TAP-tagged proteins

Except for AmiE, AmiF (lack of stability), and DnaQ (lack of TAP accessibility) all TAP-tagged proteins were purified in reasonable amounts; amounts of tagged proteins were qualitatively assessed from the gels by Coomassie Brilliant Blue staining: −, no visible protein band; +/−, visible protein band; +, high amount of protein; ++, very high amount of protein. All identified interactors are listed in supplemental Table S2. The interactome of UreA/B/G and HypB is additionally illustrated and discussed in Figs. 4–6.

ORF no.	Name	Description	Amount of purified TAP-protein	No. of identified interactors
HP0068	UreG	GTPase involved in Ni^{2+} incorporation into urease	++	33
HP0072	UreB	Urease β subunit, catalytically active subunit	++	17
HP0073	UreA	Urease α subunit	++	16
HP0197	MetK	*S*-Adenosylmethionine synthase	++	1
HP0294	AmiE	Aliphatic amidase	+/−	None
HP0516	HslU	ATP-binding subunit of heat shock protease	+	2
HP0900	HypB	GTPase involved in Ni^{2+} incorporation into hydrogenase	++	25
HP1079		ATP binding; SMC domain	+	4
HP1238	AmiF	Formamidase	+/−	None
HP1387	DnaQ	ϵ subunit of the DNA polymerase III	−	None
HP1399	RocF	Arginase	+	3

in eukaryotic cells (44). For this purpose, we used the thiol-cleavable reagent DSP, a homobifunctional cross-linker (45), that reacts with primary amines, *i.e.* lysine residues or the N terminus of proteins in near proximity (1.2 nm, ~8 atoms). The generated disulfide bridges act as conditionally covalent bonds that can be reduced by DTT, releasing the components of the purified complex before polyacrylamide gel electrophoresis. Because the natively trapped complexes are covalently cross-linked by disulfide bridges, elution from the first column by TEV cleavage was not possible because its activity requires DTT, which would result in breakage of the complexes. Instead the cross-linked complexes were eluted at low pH from the IgG column and retitrated to pH 7 before proceeding with the second purification step as illustrated in Fig. 2*B*. Interacting proteins that are not covalently cross-linked are lost during this harsh elution step from the IgG column.

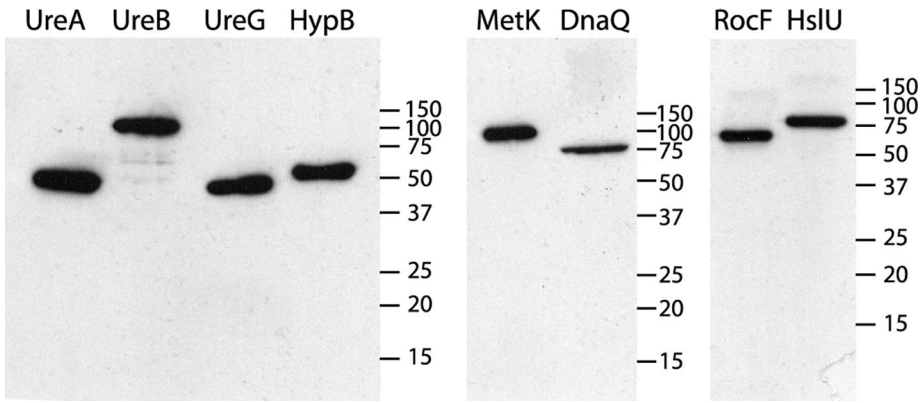

FIG. 3. **Immunoblot of crude extracts of *H. pylori* strains expressing TAP-tagged proteins using IgG.** IgG (in this case peroxidase-coupled anti-peroxidase antibody) is specifically recognized by the protein A encoded by the TAP tag in *H. pylori* protein extracts. Protein amounts were adjusted to detect the respective TAP-tagged protein (ranging from 0.5 to 10 μg). Molecular mass standards in kDa are indicated at the *right* of each blot.

We assured that cross-linking did not result in numerous unspecific interactors because we chose mild conditions, *i.e.* low concentrations of DSP (2 μg/mg of bacteria (wet weight)), a short incubation time (5 min), and low temperatures (on ice). This led to partially cross-linked cell extracts with a high number of still intact lysine residues as revealed by MALDI analysis. Therefore, our setup guaranteed the specific capturing of native complexes in whole cells and aims at establishing stringent conditions for obtaining as few false positives as possible.

For every TAP-tagged protein, we performed in parallel the classical TAP and purification after *in vivo* cross-link of complexes (Fig. 4 and supplemental Table S2). Expectedly for some proteins we had more interaction partners copurified and identified when we cross-linked before purification (supplemental Table S2). We observed that both methods, the classical TAP and the TAP after *in vivo* cross-link, were overlapping and complementary, *i.e.* we did not necessarily identify all proteins from the classical method after cross-link. Loosing interacting proteins by cross-linking is understandable considering that DSP cross-links only lysine residues or N termini of proteins in near proximity. Moreover mass spectrometry analysis is based on the tryptic digestion after lysine and arginine residues. Cross-linked proteins contain modified lysine residues that are blocked for tryptic digestion. Hence the identification of cross-linked proteins relies on the tryptic digestion after arginine and on partial cross-link of lysine residues to obtain enough peptides of a suitable size for the significant identification of the protein via mass spectrometry.

Feasibility of the TAP in H. pylori—Except for UreA-TAP and MetK-TAP, when purified by the classical strategy degradation during the purification procedure was minor for most of the TAP-tagged proteins and amounted to a maximal 5% (Fig. 4). For UreA, marginal degradation was observed when purified after *in vivo* cross-link (Fig. 4*A*). For eight TAP-tagged proteins (Table I) the criteria of stable expression and TAP accessibility for purification were fulfilled. Recurrent copurified proteins (obtained by purification using both the classical strategy and the one after *in vivo* cross-link) were considered as potential contaminants (supplemental Table S3) and withdrawn from the list of specific interactors (supplemental Table S2). We decided to attribute the status of "real interactor" to proteins that we reproducibly did not copurify with at least two baits belonging to non-overlapping protein complexes. The contaminants comprised a number of proteins previously noted as abundant in different proteomics studies (17, 46) like chaperones such as HspA and HspB (the GrosES-EL homolog), DnaK, elongation factors such as EF-TU, several ribosomal proteins, proteases, and some other highly abundant proteins (*e.g.* acetone carboxylase).

Because UreA and UreB, the two urease subunits, amount to 6% of the total *H. pylori* protein, traces of urease were detected with nearly all bait proteins and defined as contaminants. However, when urease was purified in amounts significantly higher than the contamination background (at least 2–3-fold), it was considered a true interaction.

It has to be considered that only protein bands visible after Coomassie staining were processed for mass spectrometry analysis. This increases the threshold for protein identification and improves the true positive to false positive ratio but might lead to loss of low abundance proteins.

Compared with the previous studies on the interactome of *H. pylori* using blue native two-dimensional gel or yeast two-hybrid analysis (16, 17) we found no interaction with incompatible cellular localization, *i.e.* between well defined cytoplasmic bait proteins and outer membrane or secreted proteins. This substantiates the validity of the network visualized by TAP of *H. pylori* proteins.

The complexity of the complexes obtained after TAP was variable. Relatively few interactors were obtained for MetK, HslU, HP1079, and RocF; however, these data were kept for further analysis because they reinforced the specificity of the results of the other purifications, and they allowed us to have a better insight in the recurrent contaminants obtained with TAP in *H. pylori*. In contrast, complex and highly informative complexes were obtained with the four proteins UreA, UreB, UreG, and HypB. We will focus on the analysis of these latter complexes, in particular the interactors, (i) that can be analyzed in view of previous data or that have been validated by our work or that of others and (ii) for which

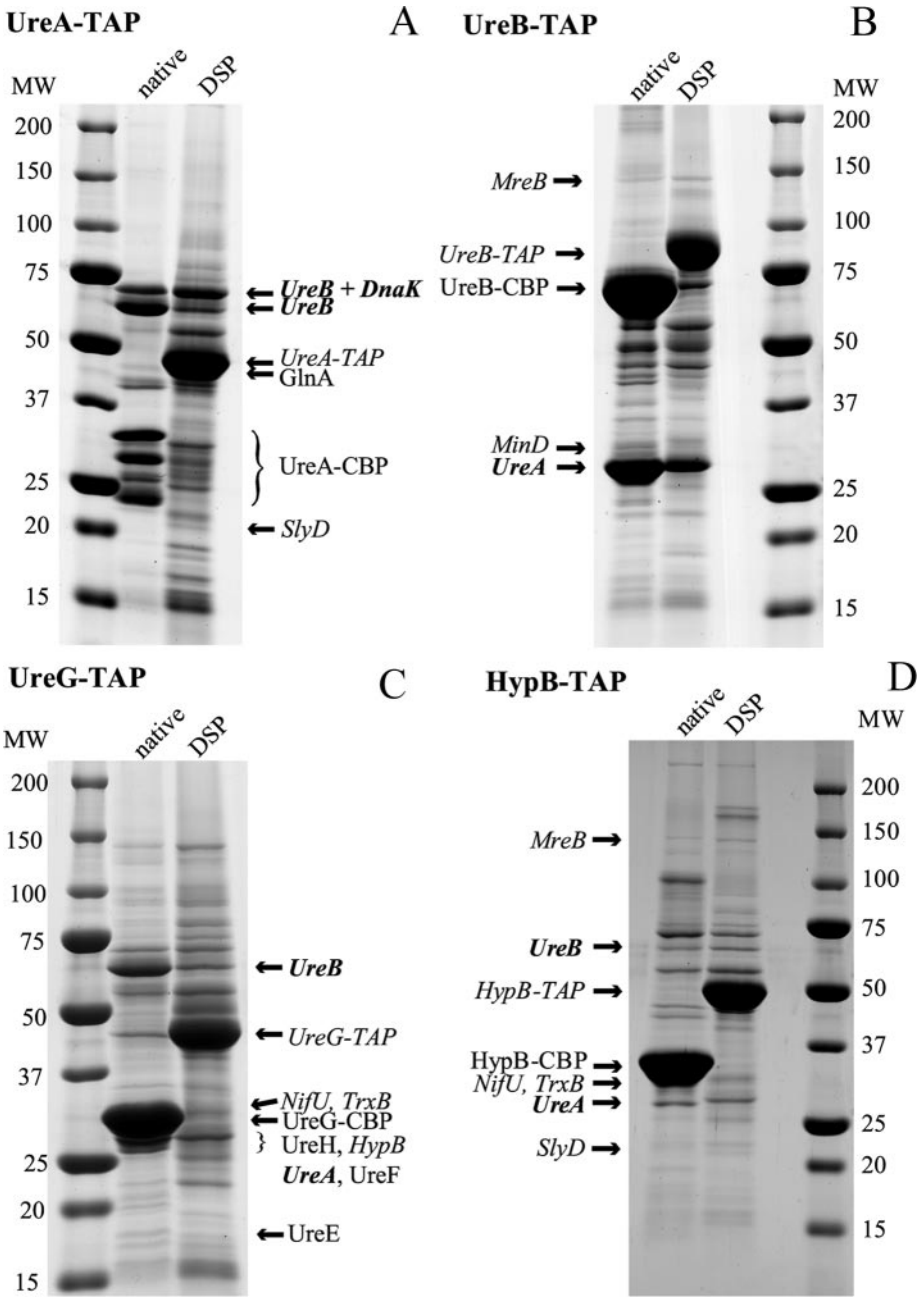

FIG. 4. **Purified protein complexes using C-terminally TAP-tagged proteins as bait.** *A*, UreA-TAP; *B*, UreB-TAP; *C*, UreG-TAP; *D*, HypB-TAP. *Left lanes*, purification under native conditions; *right lanes* (DSP), purification after cross-link in whole cells. The molecular mass is indicated in kDa. Some interactors discussed in this study are highlighted by *arrows*; *regular font*, identified interactors after native purification; *italic font*, identified interactors after cross-link purification; *bold italic font*, identified interactors in both purification procedures. "*Bait protein*"-*CBP*, target protein after TEV cleavage that is still fused to the calmodulin-binding protein.

we can propose an interpretation that could be tested in future work.

Proof of Principle: Identification of the Urease-Accessory Protein Complex—To validate our approach we decided to use one of the urease accessory proteins, UreG, as a bait because the multicomponent complex for nickel insertion into urease is well studied. UreG is a GTPase involved in Ni^{2+} incorporation into the apoenzyme, leading to enzymatic activation of urease. Using UreG as a bait protein, we purified a "complete" metallocenter biosynthesis complex composed of the structural subunits, UreA and UreB, and all accessory proteins (UreE, UreF, and UreH) required for nickel incorporation (Fig. 4*C*, Fig. 5, and supplemental Table S2). This is the first report on the purification of a urease activation complex expressed under physiological conditions. This complex is in agreement with our previous Y2H analysis that defined pairwise protein-protein interactions with some of the *H. pylori* urease proteins (16). These comprised the following interactions: UreA with UreB, UreA with UreH, UreE with UreG, and UreF with UreH; the two latter interactions were confirmed by Y2H and co-immunoprecipitation (47). Phenotypes of insertion mutations in the corresponding urease genes in *H. pylori* were in agreement with their implication in urease activation (47, 48). In addition, our data are consistent with biochemical

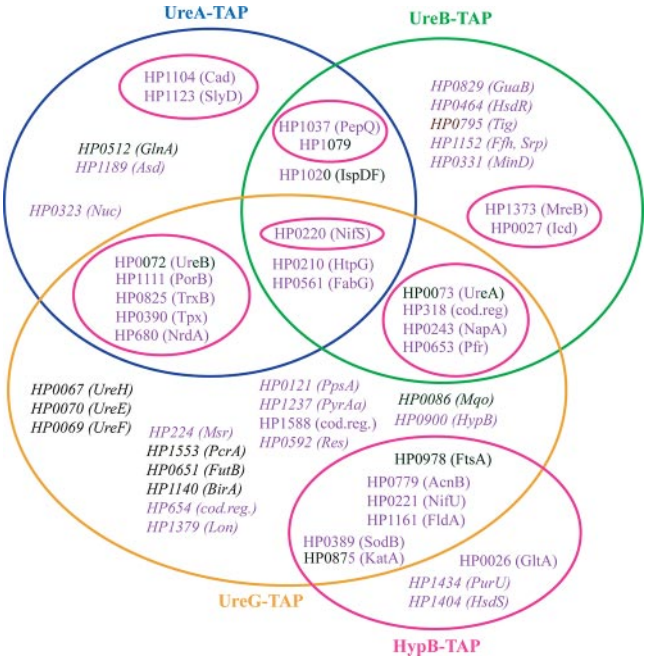

FIG. 5. **Urease and HypB interactome.** UreA, UreB, UreG, and HypB were used as TAP-tagged bait proteins. *Intersections* of *circles* illustrate overlap of interacting proteins. Font type was used as follows: *black*, identified interactors after native purification; *purple*, identified interactors using *in vivo* cross-link combined with TAP; *italics*, interactors exclusively found with the respective TAP-tagged bait. The *colors* of the *circles* around the proteins refer to the interactomes of the following baits: *blue*, UreA; *green*, UreB; *orange*, UreG; and *pink*, HypB.

data obtained for urease of *Klebsiella aerogenes*. Maturation of *K. aerogenes* urease was shown to require three accessory proteins, UreD (homolog of the *H. pylori* UreH), UreF, and UreG, and to be facilitated by UreE (5). A complex composed of *Klebsiella* apourease and UreD-UreF-UreG was suggested to be the activation-competent form of urease in the cell (6) ready to interact with UreE, a nickel-binding protein functioning as a metallochaperone that delivers nickel to urease (3). UreE was never detected in any of the isolated *Klebsiella* accessory protein-apourease complexes (4, 6); this could be interpreted to be caused by a short term interaction for nickel delivery. With the present multiprotein complex purification approach, UreE was found to be a genuine component of the *H. pylori* urease complex. However, the quantities of copurified UreE were very low, hardly visible after Coomassie staining (Fig. 4*C*); this is in agreement with a partial loss of UreE during the purification procedure.

Performing the vice versa experiment by tagging the structural subunits UreA and UreB (Figs. 4 and 5), we found reciprocally the structural partner of the urease complex but no accessory protein. The absence of accessory proteins in this complex is explainable because UreA and UreB form a very stable structural subunit complex (49), whereas the urease activation complex formed during Ni^{2+} incorporation is time-limited and was, therefore, only captured using the accessory protein UreG as a bait protein. Moreover it can be estimated that under normal growth conditions at least 75% of urease in the cell exists as the nickel-free apoenzyme (9), which is probably not interacting with the accessory proteins for nickel incorporation. However, the protein complex of UreG significantly overlapped with those of UreA and UreB (see below); this is consistent with the presence of different subpopulations of urease with partners belonging to different metabolic pathways.

Urease Is Associated with Glutamine Synthetase: Mobilization of Nitrogen from Urea—By tagging UreA we specifically found GlnA. GlnA catalyzes the synthesis of glutamine from glutamate and NH_4^+ in the presence of ATP. Glutamine is necessary for several essential metabolic pathways, such as synthesis of purine, pyrimidine, amino acids, and peptidoglycan (50). We propose that the direct physical interaction of glutamine synthetase with UreA allows the urease product, ammonium, to be directly incorporated into glutamine by the action of GlnA. "Metabolic channeling" offers unique opportunities for enhancing and regulating cellular biochemical processes. Channeling of ammonium was shown previously between the small and large subunits of carbamoyl-phosphate synthetase of *E. coli* involved in arginine and pyrimidine biosynthesis (51) and more recently in the GatCAB protein complex, a glutaminyl amidotransferase involved in ammonia transfer onto misacylated Glu-$tRNA^{Gln}$ (52). Importantly the impact of urease-derived ammonia in the nitrogen metabolism of *H. pylori* has been demonstrated by experiments showing that nitrogen from urea is indeed incorporated into amino acids in *H. pylori* (53). It is probable that the incapability of a urease-deficient strain to persist in neutralized gastric environments is, at least in part, because of an impaired nitrogen acquisition.

Interaction of the Urease Complex with Hydrogenase Accessory Proteins—When we used UreG as a bait, we found specifically HypB after *in vivo* cross-linking. HypB is a GTPase essential for Ni^{2+} incorporation into hydrogenase (54), similar to UreG for urease. Importantly HypB was not found with any other bait protein, stressing the specificity of the *in vivo* cross-link method for TAP. The intertwinement of Ni^{2+} incorporation into urease and hydrogenase had been suggested because an *H. pylori hypB*-deficient mutant exhibited significantly decreased urease activity (13). This effect was confirmed in a Δ*hypB* mutant of the strain used in the present study, 26695 (data not shown). Performing the vice versa experiment by purifying a TAP version of HypB resulted in copurification of a 2–3-fold higher amount of UreA and UreB than usually observed for background contamination (Fig. 4*D*). Hence our data provide the first *in vivo* evidence that HypB physically interacted with urease, consistent with the functional relation between the two. Recently the *in vitro* interaction of HypA with UreE, additional hydrogenase, and urease accessory proteins, respectively, was demonstrated, enriching the view of a direct physical interaction between both maturation systems for urease and hydrogenase (55).

Furthermore tagging UreA or HypB we found SlyD, a peptidyl-prolyl cis-trans isomerase involved in hydrogenase maturation (56, 57). In *E. coli*, SlyD bound nickel at its histidine-, cysteine-, and carboxyl-rich C terminus (58), and a *slyD* deletion resulted in both reduced hydrogenase activity and nickel accumulation (56). Interestingly a recent study showed that SlyD stimulated nickel release from HypB (59). In addition, SlyD was shown to interact with the Tat signal and to prevent premature export of Tat-targeted proteins (60). SlyD was isolated as the sole interactor of HypB in a study in which separate complexes of hydrogenase accessory proteins were natively copurified in *E. coli* (25). Accordingly we have found no hydrogenase or other hydrogenase accessory proteins (*e.g.* HypA) other than SlyD (25) interacting with HypB or UreA, UreB, and UreG in *H. pylori* either because of the low abundance and the transient nature of the hydrogenase maturation complex *in vivo* or because membrane-associated proteins like the hydrogenase are lost during TAP.

Overlap of the Interactomes of Urease and HypB: Interaction with Components of the Cytoskeleton—Analysis of the interactome of HypB revealed a remarkable overlap of interacting proteins with the urease complex. These comprised several proteins of the bacterial cytoskeleton. UreG and HypB were copurified with the cell division protein FtsA, an actin homolog involved in cell division. UreB and HypB copurified with another bacterial actin-like protein MreB, and UreB additionally interacted with the cell division inhibitor protein MinD (Fig. 5). In addition, we identified HP1079, a protein of unknown function harboring an SMC (structural maintenance of chromosomes) motif as a component of the interactome of urease and HypB. It can be envisioned that the small proportion of activated urease is sequestered in a compartment of the cell to improve its activity in connection for instance with the ammonium-incorporating enzyme, glutamine synthetase, under conditions of normal growth or with the urea inner membrane channel, UreI, for efficient substrate delivery upon acid stress. Accordingly a UreI-dependent membrane association of urease was reported previously (47, 61).

Interactions with Housekeeping [Fe-S] Cluster Assembly Proteins—The interactomes of HypB and urease additionally included proteins involved in the formation of [Fe-S] clusters. Among them, we found NifS and NifU, representing the sole system for [Fe-S] cluster formation in *H. pylori* (62) that are essential for survival of the pathogen (63). NifS provides sulfur via cysteine desulfurase activity, whereas NifU is a scaffold protein onto which the nascent [Fe-S] cluster is assembled. Furthermore the thioredoxin reductase TrxB was copurified. TrxB was demonstrated to mediate iron binding of IscA and delivery to IscU, two *E. coli* proteins analogous to NifS and NifU, respectively (64). Therefore, we predict that TrxB is involved in iron binding to NifS and delivery to NifU in *H. pylori*. Furthermore we copurified with HypB, UreG, and UreB two iron storage proteins, NapA and the Pfr ferritin (65, 66). In *Salmonella enterica* sv. Typhimurium, ferritin B has been shown to represent a major iron donor for iron-sulfur cluster repair (67). In addition, we copurified flavodoxin, a low potential electron donor for a number of redox enzymes using HypB and UreG as bait proteins. Because flavodoxin is likely not to be involved as electron acceptor of hydrogenase, as shown for its homologue from *Wolinella succinogenes* (68), a potential role for flavodoxin in intermediate electron transfer for maturation of [Fe-S] clusters in *H. pylori* needs to be examined. We also captured aconitase B, a paradigmatic [Fe-S]-containing protein, with HypB and UreG. The association of aconitase B with this complex might be related with the extreme vulnerability of one of its [Fe-S] clusters to oxidation that is known to require frequent repair (69). Taken together, our data indicated that we indeed captured proteins implicated in the housekeeping [Fe-S] cluster assembly and regeneration in *H. pylori*.

The *H. pylori* hydrogenase belongs to the family of [NiFe] hydrogenases that consist of two subunits and a metal-containing catalytic site, which is assembled by complex mechanisms (12, 70). The large subunit (HydB) contains a dinuclear catalytic center composed of a nickel ion bound to four cysteine residues, two of which are linked to an iron ion. Iron of the Ni/Fe metallocenter is probably provided by the consecutive action of HypE and HypF, preparing the cyanid ligands from carbamoyl phosphate (71–73) and then delivering them to a HypD-HypC complex that inserts the iron center (74). The small subunit (HydA) carries three [Fe-S] clusters that form a conduit for electron transfer to the appropriate carrier (75). Because *H. pylori* lacks HupGHIJ shown to be implicated in maturation of the small hydrogenase subunit in *Rhizobium leguminosarum* (76), it is tentative to propose that the housekeeping [Fe-S] cluster assembly and insertion system, Nif, is involved in maturation of the small hydrogenase subunit in *H. pylori*.

Spatiotemporal Insights into the Maturation of Hydrogenase—HypB is involved in nickel incorporation into the Ni/Fe site located in the large subunit of hydrogenase, whereas [Fe-S] clusters are situated in the small subunit. Taking together our TAP data and the crystal structure of hydrogenase from *Desulfovibrio gigas* (75), it is possible that HypB is located in near proximity to the [Fe-S] clusters of the small subunit upon its action on nickel delivery to the large hydrogenase subunit once the heterodimer is formed.

We propose a model for sequential activation and export of hydrogenase (Fig. 7) in which the large and the small subunit form a membrane-bound apoheterodimer in association with the twin arginine export system after cytoplasmic incorporation of iron into the large subunit. In the cytoplasm, a precomplex for "late maturation" of hydrogenase is formed that comprises HypAB, SlyD, and proteins of the Nif system. Concomitantly [Fe-S] clusters are formed in the small subunit by the action of the Nif system, and nickel is provided for the large subunit by HypAB and SlyD. To our knowledge, this model integrates all current data about maturation of periplas-

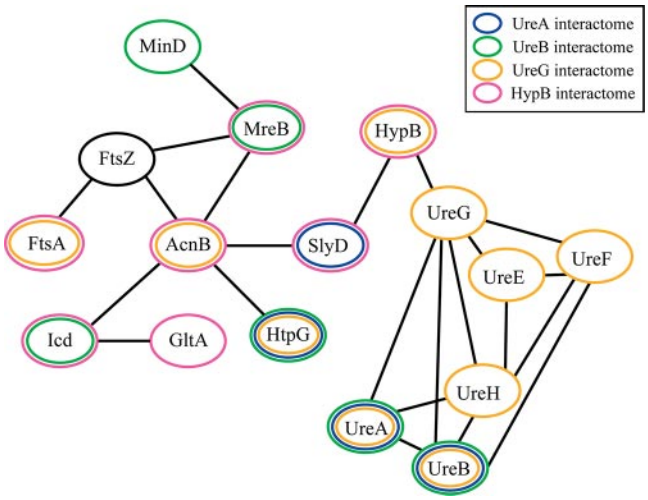

FIG. 6. **Comparison of the *H. pylori* interactome with the STRING data.** The predicted functional associations that were found both in our study and in the STRING interaction database restricted to the highly significant categories co-occurrence and experiments are illustrated as a network. The *colors* of the *circles* around the proteins refer to the interactomes of the present study with the following baits: *blue*, UreA; *green*, UreB; *orange*, UreG; and *pink*, HypB. The *black circled* interactor was only predicted in the STRING database; from the total amount of interactors, nearly one-third was in common with STRING predictions.

mic [NiFe] hydrogenase. First, the observation of a dynamic complex of HypCDEF (74) and the interaction of HypC with HypD and with the large hydrogenase subunit (25) indicate a cytoplasmic preinsertion of iron into the large subunit in the absence of nickel-inserting proteins. Second, because membrane-associated proteins are lost during TAP, it explains (with the exception of loss of HypA) why purifying HypB did not result in copurification of hydrogenase or other hydrogenase accessory proteins other than SlyD (Ref. 25 and our results). Third, SlyD was shown to interact with the Tat signal and to prevent premature export of Tat-targeted proteins (60). Therefore, by dual interaction with HypB and the Tat signal sequence of the small hydrogenase subunit, SlyD might link timing of nickel insertion to export of holohydrogenase into the periplasm.

Comparison of Our Interactome Networks with Available Bacterial Protein-Protein Interaction Data—Comparing our results with the Y2H data (16) and considering only direct interactions, we exclusively found overlap in the urease maturation complex. The Y2H approach usually results in a high number of false positives and includes data of "promiscuous" or "sticky" proteins (77). This leads to a highly connected and, therefore, meaningless network when second- or third-order interactions are considered (own observation using PIMrider (Hybrigenics) for *H. pylori*). In *Saccharomyces cerevisiae* pro-

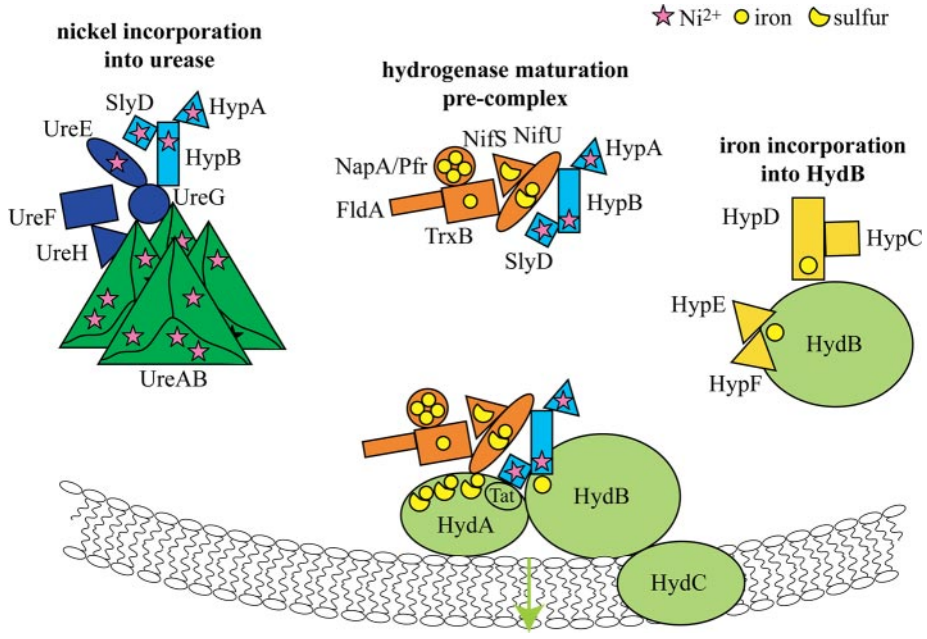

FIG. 7. **Model for metal incorporation into urease and hydrogenase in *H. pylori*.** Incorporation of nickel into urease is restricted to the cytoplasm and involves the hydrogenase accessory proteins HypA, HypB, and SlyD (which except for HypA are all components purified in this study). Maturation of hydrogenase is mediated by temporally and spatially separated complexes. A cytosolic complex composed of HypCDEF mediates incorporation of iron into the large hydrogenase subunit, HydB (74) (not purified here). A second cytosolic precomplex consists of the nickel-incorporating proteins, HypA, HypB, and SlyD, and proteins involved in [Fe-S] cluster formation (except for HypA all components were purified in this study). Upon nickel availability, this precomplex interacts with a heterocomplex of apoHydA and iron-containing HydB at the membrane and concomitantly incorporates nickel into HydB and forms [Fe-S] clusters in HydA. In this model, export of maturated hydrogenase via the twin arginine system is timely coordinated by the dual interaction of SlyD with HypB and with the Tat signal of the small hydrogenase subunit.

tein-protein interactions were monitored by both Y2H and TAP methods, and comparison of the results revealed that the tandem purification was more reliable and better predicted protein functions (19). Analyses of *H. pylori* protein complexes by blue native two-dimensional gel electrophoresis (17) are difficult to interpret because the resolution of the gels is limited, and hence the definition of a complex is relatively subjective. The authors of the latter study identified 13 multicomplexes among which the only overlap was UreA-UreB.

We searched to confront our interactome with the protein-protein interaction data from a variety of sources that are available online at the STRING database ("search tool for the retrieval of interacting genes/proteins" (78)). The underlying infrastructure of this database includes a consistent body of completely sequenced genomes (currently 373 species) and exhaustive orthology classifications based on which interaction evidence is transferred between organisms. This resource integrates both predicted and known interactions (among which is the large scale *E. coli* interactome of Butland *et al.* (24)) that were based and classified on different criteria. To compare these data with our interactome results, we exclusively took into account two highly stringent STRING criteria, namely "co-occurrence" based on the observation that functionally associated proteins have similar phylogenetic distribution profiles and "experiments," *i.e.* experimentally proven interactions from published studies. Results from four baits, UreA, UreB, UreG, and HypB (supplemental Table S2), were compared with those predicted by STRING. Functional associations predicted by STRING that were in common with our interactome data are depicted in Fig. 6. We found a 29% coverage of our multicomplex data with STRING, indicating that our approach is, first of all, consistent with previous highly significant data but also largely extends the view on the interactome of the chosen bait proteins.

Conclusions—To monitor functional protein associations in *H. pylori*, we established the TAP technique in the gastric pathogen and combined this method with *in vivo* cross-link for capturing transient interactions.

We were able to purify the whole nickel incorporation complex of urease. Furthermore urease was associated with glutamine synthetase, suggesting that production and assimilation of ammonium is coupled. Interactions between urease and the cytoskeleton have also been observed for the first time, which raises questions about the cellular compartmentalization of the low amount of activated urease to maximize metabolic coupling (*e.g.* incorporation of ammonium into amino acids and other components). In addition, several new interaction partners not discussed here open up entirely new fields of study; some of them are under investigation. We identified for the first time a physical interaction between the urease and the hydrogenase accessory protein HypB *in vivo*, suggesting a competition for nickel ions during incorporation. Purification of the complete urease maturation complex but only of parts of the hydrogenase maturation complex is likely due to the fact that maturation of urease exclusively takes place in the cytoplasm, whereas hydrogenase maturation is at least temporally coupled to the membrane via the twin arginine export system. We propose a model (Fig. 7) in which nickel is coordinately distributed to two essential enzymes, either urease, which is necessary for acid resistance and possibly ammonium assimilation, or hydrogenase, which is important for energy supply.

Acknowledgments—We thank Cosmin Saveanu, Alain Jacquier, Ivo G. Boneca, Anna Pawlik, and Damien Leduc for constant interest in this project and for many helpful discussions.

* This work was supported in part by Programmes Transversaux de Recheche (PTR) funding of the Institut Pasteur (Grant PTR 184). The costs of publication of this article were defrayed in part by the payment of page charges. This article must therefore be hereby marked "*advertisement*" in accordance with 18 U.S.C. Section 1734 solely to indicate this fact.

S The on-line version of this article (available at http://www.mcponline.org) contains supplemental material.

¶ Supported by subsequent postdoctoral fellowships of the German Academic Exchange Service (DAAD) and the Fondation pour la Recherche Médicale (FRM). To whom correspondence may be addressed: Westfälische Wilhelms-Universität Münster, Inst. für Allgemeine Zoologie und Genetik, Schlossplatz 5, 48149 Münster, Germany. Tel.: 49-251-83-23-926; Fax: 49-251-83-24-723; E-mail: kerstin.stingl@uni-muenster.de.

** Supported by the DAAD. Present address: Subcellular structure and cellular dynamics, UMR 144 CNRS, Inst. Curie, F-75005 Paris Cedex, France.

¶¶ To whom correspondence may be addressed: Inst. Pasteur, Unité Postulante de Pathogenèse de *Helicobacter*, 28 rue du Docteur Roux, F-75015 Paris Cedex, France. Tel.: 33-1-40-61-36-41; Fax: 33-1-40-61-36-40; E-mail: hdereuse@pasteur.fr.

REFERENCES

1. Ernst, P. B., and Gold, B. D. (2000) The disease spectrum of *Helicobacter pylori*: the immunopathogenesis of gastroduodenal ulcer and gastric cancer. *Annu. Rev. Microbiol.* **54,** 615–640
2. Marshall, B. J., Barrett, L. J., Prakash, C., McCallum, R. W., and Guerrant, R. L. (1990) Urea protects *Helicobacter* (*Campylobacter*) *pylori* from the bactericidal effect of acid. *Gastroenterology* **99,** 697–702
3. Colpas, G. J., and Hausinger, R. P. (2000) In vivo and in vitro kinetics of metal transfer by the *Klebsiella aerogenes* urease nickel metallochaperone, UreE. *J. Biol. Chem.* **275,** 10731–10737
4. Brayman, T. G., and Hausinger, R. P. (1996) Purification, characterization, and functional analysis of a truncated *Klebsiella aerogenes* UreE urease accessory protein lacking the histidine-rich carboxyl terminus. *J. Bacteriol.* **178,** 5410–5416
5. Lee, M. H., Mulrooney, S. B., Renner, M. J., Markowicz, Y., and Hausinger, R. P. (1992) Klebsiella aerogenes urease gene cluster: sequence of ureD and demonstration that four accessory genes (ureD, ureE, ureF, and ureG) are involved in nickel metallocenter biosynthesis. *J. Bacteriol.* **174,** 4324–4330
6. Park, I. S., and Hausinger, R. P. (1995) Evidence for the presence of urease apoprotein complexes containing UreD, UreF, and UreG in cells that are competent for in vivo enzyme activation. *J. Bacteriol.* **177,** 1947–1951
7. Soriano, A., and Hausinger, R. P. (1999) GTP-dependent activation of urease apoprotein in complex with the UreD, UreF, and UreG accessory proteins. *Proc. Natl. Acad. Sci. U. S. A.* **96,** 11140–11144
8. Mulrooney, S. B., Ward, S. K., and Hausinger, R. P. (2005) Purification and properties of the *Klebsiella aerogenes* UreE metal-binding domain, a functional metallochaperone of urease. *J. Bacteriol.* **187,** 3581–3585
9. Stingl, K., and De Reuse, H. (2005) Staying alive overdosed: how does *Helicobacter pylori* control urease activity? *Int. J. Med. Microbiol.*

295, 307–315
10. Eaton, K. A., and Krakowka, S. (1994) Effect of gastric pH on urease-dependent colonization of gnotobiotic piglets by *Helicobacter pylori*. *Infect. Immun.* **62,** 3604–3607
11. Olson, J. W., and Maier, R. J. (2002) Molecular hydrogen as an energy source for *Helicobacter pylori*. *Science* **298,** 1788–1790
12. Leach, M. R., and Zamble, D. B. (2007) Metallocenter assembly of the hydrogenase enzymes. *Curr. Opin. Chem. Biol.* **11,** 159–165
13. Olson, J. W., Mehta, N. S., and Maier, R. J. (2001) Requirement of nickel metabolism proteins HypA and HypB for full activity of both hydrogenase and urease in *Helicobacter pylori*. *Mol. Microbiol.* **39,** 176–182
14. Rual, J. F., Venkatesan, K., Hao, T., Hirozane-Kishikawa, T., Dricot, A., Li, N., Berriz, G. F., Gibbons, F. D., Dreze, M., Ayivi-Guedehoussou, N., Klitgord, N., Simon, C., Boxem, M., Milstein, S., Rosenberg, J., Goldberg, D. S., Zhang, L. V., Wong, S. L., Franklin, G., Li, S., Albala, J. S., Lim, J., Fraughton, C., Llamosas, E., Cevik, S., Bex, C., Lamesch, P., Sikorski, R. S., Vandenhaute, J., Zoghbi, H. Y., Smolyar, A., Bosak, S., Sequerra, R., Doucette-Stamm, L., Cusick, M. E., Hill, D. E., Roth, F. P., and Vidal, M. (2005) Towards a proteome-scale map of the human protein-protein interaction network. *Nature* **437,** 1173–1178
15. Legrain, P., Wojcik, J., and Gauthier, J. M. (2001) Protein-protein interaction maps: a lead towards cellular functions. *Trends Genet.* **17,** 346–352
16. Rain, J. C., Selig, L., De Reuse, H., Battaglia, V., Reverdy, C., Simon, S., Lenzen, G., Petel, F., Wojcik, J., Schächter, V., Chemama, Y., Labigne, A., and Legrain, P. (2001) The protein-protein interaction map of *Helicobacter pylori*. *Nature* **409,** 211–215
17. Pyndiah, S., Lasserre, J. P., Menard, A., Claverol, S., Prouzet-Mauleon, V., Megraud, F., Zerbib, F., and Bonneu, M. (2007) Two-dimensional blue native/SDS gel electrophoresis of multiprotein complexes from *Helicobacter pylori*. *Mol. Cell. Proteomics* **6,** 193–206
18. Rigaut, G., Shevchenko, A., Rutz, B., Wilm, M., Mann, M., and Séraphin, B. (1999) A generic protein purification method for protein complex characterization and proteome exploration. *Nat. Biotechnol.* **17,** 1030–1032
19. Deng, M., Sun, F., and Chen, T. (2003) Assessment of the reliability of protein-protein interactions and protein function prediction. *Eight Pac. Symp. Biocomput*. 140–151
20. von Mering, C., Krause, R., Snel, B., Cornell, M., Oliver, S. G., Fields, S., and Bork, P. (2002) Comparative assessment of large-scale data sets of protein-protein interactions. *Nature* **417,** 399–403
21. Gavin, A. C., Bosche, M., Krause, R., Grandi, P., Marzioch, M., Bauer, A., Schultz, J., Rick, J. M., Michon, A. M., Cruciat, C. M., Remor, M., Hofert, C., Schelder, M., Brajenovic, M., Ruffner, H., Merino, A., Klein, K., Hudak, M., Dickson, D., Rudi, T., Gnau, V., Bauch, A., Bastuck, S., Huhse, B., Leutwein, C., Heurtier, M. A., Copley, R. R., Edelmann, A., Querfurth, E., Rybin, V., Drewes, G., Raida, M., Bouwmeester, T., Bork, P., Seraphin, B., Kuster, B., Neubauer, G., and Superti-Furga, G. (2002) Functional organization of the yeast proteome by systematic analysis of protein complexes. *Nature* **415,** 141–147
22. Van Leene, J., Stals, H., Eeckhout, D., Persiau, G., Van Slijke, E., Van Isterdael, G., De Clercq, A., Bonnet, E., Laukens, K., Remmerie, N., Hendrickx, K., De Vijlder, T., Adbelkrim, A., Pharazyn, A., Van Onckelen, H., Inze, D., Witters, E., and De Jaeger, G. (2007) A tandem affinity purification-based technology platform to study the cell cycle interactome in *Arabidopsis thaliana*. *Mol. Cell. Proteomics* **6,** 1226–1238
23. Koch, H. B., Zhang, R., Verdoodt, B., Bailey, A., Zhang, C. D., Yates, J. R., III, Menssen, A., and Hermeking, H. (2007) Large-scale identification of c-MYC-associated proteins using a combined TAP/MudPIT approach. *Cell Cycle* **6,** 205–217
24. Butland, G., Peregrin-Alvarez, J. M., Li, J., Yang, W., Yang, X., Canadien, V., Starostine, A., Richards, D., Beattie, B., Krogan, N., Davey, M., Parkinson, J., Greenblatt, J., and Emili, A. (2005) Interaction network containing conserved and essential protein complexes in Escherichia coli. *Nature* **433,** 531–537
25. Butland, G., Zhang, J. W., Yang, W., Sheung, A., Wong, P., Greenblatt, J. F., Emili, A., and Zamble, D. B. (2006) Interactions of the *Escherichia coli* hydrogenase biosynthetic proteins: HybG complex formation. *FEBS Lett.* **580,** 677–681
26. Gully, D., and Bouveret, E. (2006) A protein network for phospholipid synthesis uncovered by a variant of the tandem affinity purification method in *Escherichia coli*. *Proteomics* **6,** 282–293
27. Gully, D., Moinier, D., Loiseau, L., and Bouveret, E. (2003) New partners of acyl carrier protein detected in *Escherichia coli* by tandem affinity purification. *FEBS Lett.* **548,** 90–96
28. Kumar, J. K., Tabor, S., and Richardson, C. C. (2004) Proteomic analysis of thioredoxin-targeted proteins in *Escherichia coli*. *Proc. Natl. Acad. Sci. U. S. A.* **101,** 3759–3764
29. Casadaban, M. J., and Cohen, S. N. (1980) Analysis of gene control signals by DNA fusion and cloning in *Escherichia coli*. *J. Mol. Biol.* **138,** 179–207
30. Miller, J. F. (1992) *A Short Course in Bacterial Genetics: A Laboratory Manual and Handbook for Escherichia coli and Related Bacteria*, Cold Spring Harbor Laboratory Press, Cold Spring Harbor, NY
31. Bury-Moné, S., Skouloubris, S., Dauga, C., Thiberge, J.-M., Dailidiene, D., Berg, D. E., Labigne, A., and De Reuse, H. (2003) Presence of active aliphatic amidases in *Helicobacter* species able to colonize the stomach. *Infect. Immun.* **71,** 5613–5622
32. Menard, R., Sansonetti, P. J., and Parsot, C. (1993) Nonpolar mutagenesis of the *ipa* genes defines IpaB, IpaC, and IpaD as effectors of *Shigella flexneri* entry into epithelial cells. *J. Bacteriol.* **175,** 5899–5906
33. Colland, F., Rain, J. C., Gounon, P., Labigne, A., Legrain, P., and De Reuse, H. (2001) Identification of the *Helicobacter pylori* anti-sigma28 factor. *Mol. Microbiol.* **41,** 477–487
34. Neuhoff, V., Arold, N., Taube, D., and Ehrhardt, W. (1988) Improved staining of proteins in polyacrylamide gels including isoelectric focusing gels with clear background at nanogram sensitivity using Coomassie Brilliant Blue G-250 and R-250. *Electrophoresis* **9,** 255–262
35. Boneca, I. G., de Reuse, H., Epinat, J. C., Pupin, M., Labigne, A., and Moszer, I. (2003) A revised annotation and comparative analysis of *Helicobacter pylori* genomes. *Nucleic Acids Res.* **31,** 1704–1714
36. Skouloubris, S., Thiberge, J. M., Labigne, A., and De Reuse, H. (1998) The *Helicobacter pylori* UreI protein is not involved in urease activity but is essential for bacterial survival *in vivo*. *Infect. Immun.* **66,** 4517–4521
37. Tomb, J. F., White, O., Kerlavage, A. R., Clayton, R. A., Sutton, G. G., Fleischmann, R. D., Ketchum, K. A., Klenk, H. P., Gill, S., Dougherty, B. A., Nelson, K., Quackenbush, J., Zhou, L., Kirkness, E. F., Peterson, S., Loftus, B., Richardson, D., Dodson, R., Khalak, H. G., Glodek, A., McKenney, K., Fitzegerald, L. M., Lee, N., Adams, M. D., and Venter, J. C. (1997) The complete genome sequence of the gastric pathogen *Helicobacter pylori*. *Nature* **388,** 539–547
38. McGee, D. J., Radcliff, F. J., Mendz, G. L., Ferrero, R. L., and Mobley, H. L. T. (1999) Helicobacter pylori rocF is required for arginase activity and acid protection *in vitro* but is not essential for colonization of mice or for urease activity. *J. Bacteriol.* **181,** 7314–7322
39. Skouloubris, S., Labigne, A., and De Reuse, H. (2001) The AmiE aliphatic amidase and AmiF formamidase of *Helicobacter pylori*: natural evolution of two enzyme paralogues. *Mol. Microbiol.* **40,** 596–609
40. Bury-Moné, S., Thiberge, J.-M., Contreras, M., Maitournam, A., Labigne, A., and De Reuse, H. (2004) Responsiveness to acidity via metal ion regulators mediates virulence in the gastric pathogen *Helicobacter pylori*. *Mol. Microbiol.* **53,** 623–638
41. Zeghouf, M., Li, J., Butland, G., Borkowska, A., Canadien, V., Richards, D., Beattie, B., Emili, A., and Greenblatt, J. F. (2004) Sequential peptide affinity (SPA) system for the identification of mammalian and bacterial protein complexes. *J. Proteome Res.* **3,** 463–468
42. Zawilak-Pawlik, A., Kois, A., Stingl, K., Boneca, I. G., Skrobuk, P., Piotr, J., Lurz, R., Zakrzewska-Czerwinska, J., and Labigne, A. (2007) HobA—a novel protein involved in initiation of chromosomal replication in *Helicobacter pylori*. *Mol. Microbiol.* **65,** 979–994
43. Schauer, K., Gouget, B., Carriere, M., Labigne, A., and de Reuse, H. (2007) Novel nickel transport mechanism across the bacterial outer membrane energized by the TonB/ExbB/ExbD machinery. *Mol. Microbiol.* **63,** 1054–1068
44. Vasilescu, J., Guo, X., and Kast, J. (2004) Identification of protein-protein interactions using *in vivo* cross-linking and mass spectrometry. *Proteomics* **4,** 3845–3854
45. Lomant, A. J., and Fairbanks, G. (1976) Chemical probes of extended biological structures: synthesis and properties of the cleavable protein cross-linking reagent [^{35}S]dithiobis(succinimidyl propionate). *J. Mol. Biol.* **104,** 243–261
46. Bumann, D., Meyer, T. F., and Jungblut, P. R. (2001) Proteome analysis of the common human pathogen *Helicobacter pylori*. *Proteomics* **1,** 473–479
47. Voland, P., Weeks, D. L., Marcus, E. A., Prinz, C., Sachs, G., and Scott, D.

(2003) Interactions among the seven *Helicobacter pylori* proteins encoded by the urease gene cluster. *Am. J. Physiol.* **284,** G96–G106
48. Cussac, V., Ferrero, R. L., and Labigne, A. (1992) Expression of *Helicobacter pylori* urease genes in *Escherichia coli* grown under nitrogen-limiting conditions. *J. Bacteriol.* **174,** 2466–2473
49. Ha, N. C., Oh, S. T., Sung, J. Y., Cha, K. A., Lee, M. H., and Oh, B. H. (2001) Supramolecular assembly and acid resistance of *Helicobacter pylori* urease. *Nat. Struct. Biol.* **8,** 505–509
50. Reitzer, L. J. (1996) Ammonia assimilation and the biosynthesis of glutamine, glutamate, aspartate, asparagine, L-alanine and D-alanine, in *Escherichia coli and Salmonella: Cellular and Molecular Biology* (Neidhardt, F. C., Curtiss, R., Ingraham, J. L., Lin, E. C. C., Low, K. B., Magasanik, B., Riley, M., Schaechter, M., and Umbarger, H. E., eds) 2nd Ed., pp. 391–407, American Society for Microbiology (ASM) Press, Washington, DC
51. Thoden, J. B., Holden, H. M., Wesenberg, G., Raushel, F. M., and Rayment, I. (1997) Structure of carbamoyl phosphate synthetase: a journey of 96 A from substrate to product. *Biochemistry* **36,** 6305–6316
52. Nakamura, A., Yao, M., Chimnaronk, S., Sakai, N., and Tanaka, I. (2006) Ammonia channel couples glutaminase with transamidase reactions in GatCAB. *Science* **312,** 1954–1958
53. Williams, C. L., Preston, T., Hossack, M., Slater, C., and McColl, K. E. (1996) Helicobacter pylori utilises urea for amino acid synthesis. *FEMS Immunol. Med. Microbiol.* **13,** 87–94
54. Maier, T., Jacobi, A., Sauter, M., and Bock, A. (1993) The product of the *hypB* gene, which is required for nickel incorporation into hydrogenases, is a novel guanine nucleotide-binding protein. *J. Bacteriol.* **175,** 630–635
55. Benoit, S. L., Mehta, N., Weinberg, M. V., Maier, C., and Maier, R. J. (2007) Interaction between the *Helicobacter pylori* accessory proteins HypA and UreE is needed for urease maturation. *Microbiology* **153,** 1474–1482
56. Zhang, J. W., Butland, G., Greenblatt, J. F., Emili, A., and Zamble, D. B. (2005) A role for SlyD in the *Escherichia coli* hydrogenase biosynthetic pathway. *J. Biol. Chem.* **280,** 4360–4366
57. Scholz, C., Eckert, B., Hagn, F., Schaarschmidt, P., Balbach, J., and Schmid, F. X. (2006) SlyD proteins from different species exhibit high prolyl isomerase and chaperone activities. *Biochemistry* **45,** 20–33
58. Hottenrott, S., Schumann, T., Pluckthun, A., Fischer, G., and Rahfeld, J. U. (1997) The *Escherichia coli* SlyD is a metal ion-regulated peptidyl-prolyl cis/trans-isomerase. *J. Biol. Chem.* **272,** 15697–15701
59. Leach, M. R., Zhang, J. W., and Zamble, D. B. (2007) The role of complex formation between the *Escherichia coli* hydrogenase accessory factors HypB and SlyD. *J. Biol. Chem.* **282,** 16177–16186
60. Graubner, W., Schierhorn, A., and Bruser, T. (2007) DnaK plays a pivotal role in Tat targeting of CueO and functions beside SlyD as a general Tat signal binding chaperone. *J. Biol. Chem.* **282,** 7116–7124
61. Hong, W., Sano, K., Morimatsu, S., Scott, D. R., Weeks, D. L., Sachs, G., Goto, T., Mohan, S., Harada, F., Nakajima, N., and Nakano, T. (2003) Medium pH-dependent redistribution of the urease of *Helicobacter pylori. J. Med. Microbiol.* **52,** 211–216
62. Tokumoto, U., Kitamura, S., Fukuyama, K., and Takahashi, Y. (2004) Interchangeability and distinct properties of bacterial Fe-S cluster assembly systems: functional replacement of the *isc* and *suf* operons in *Escherichia coli* with the *nifSU*-like operon from *Helicobacter pylori. J. Biochem.* (*Tokyo*) **136,** 199–209
63. Olson, J. W., Agar, J. N., Johnson, M. K., and Maier, R. J. (2000) Characterization of the NifU and NifS Fe-S cluster formation proteins essential for viability in *Helicobacter pylori. Biochemistry* **39,** 16213–16219
64. Ding, H., Harrison, K., and Lu, J. (2005) Thioredoxin reductase system mediates iron binding in IscA and iron delivery for the iron-sulfur cluster assembly in IscU. *J. Biol. Chem.* **280,** 30432–30437
65. Bereswill, S., Waidner, U., Odenbreit, S., Lichte, F., Fassbinder, F., Bode, G., and Kist, M. (1998) Structural, functional and mutational analysis of the *pfr* gene encoding a ferritin from *Helicobacter pylori. Microbiology* **144,** 2505–2516
66. Tonello, F., Dundon, W. G., Satin, B., Molinari, M., Tognon, G., Grandi, G., Del Giudice, G., Rappuoli, R., and Montecucco, C. (1999) The *Helicobacter pylori* neutrophil-activating protein is an iron-binding protein with dodecameric structure. *Mol. Microbiol.* **34,** 238–246
67. Velayudhan, J., Castor, M., Richardson, A., Main-Hester, K. L., and Fang, F. C. (2007) The role of ferritins in the physiology of *Salmonella enterica* sv. Typhimurium: a unique role for ferritin B in iron-sulphur cluster repair and virulence. *Mol. Microbiol.* **63,** 1495–1507
68. Biel, S., Klimmek, O., Gross, R., and Kroger, A. (1996) Flavodoxin from Wolinella succinogenes. *Arch. Microbiol.* **166,** 122–127
69. Gardner, P. R. (2002) Aconitase: sensitive target and measure of superoxide. *Methods Enzymol.* **349,** 9–23
70. Kuchar, J., and Hausinger, R. P. (2004) Biosynthesis of metal sites. *Chem. Rev.* **104,** 509–525
71. Paschos, A., Bauer, A., Zimmermann, A., Zehelein, E., and Bock, A. (2002) HypF, a carbamoyl phosphate-converting enzyme involved in [NiFe] hydrogenase maturation. *J. Biol. Chem.* **277,** 49945–49951
72. Reissmann, S., Hochleitner, E., Wang, H., Paschos, A., Lottspeich, F., Glass, R. S., and Bock, A. (2003) Taming of a poison: biosynthesis of the NiFe-hydrogenase cyanide ligands. *Science* **299,** 1067–1070
73. Blokesch, M., Paschos, A., Bauer, A., Reissmann, S., Drapal, N., and Bock, A. (2004) Analysis of the transcarbamoylation-dehydration reaction catalyzed by the hydrogenase maturation proteins HypF and HypE. *Eur. J. Biochem.* **271,** 3428–3436
74. Blokesch, M., Albracht, S. P., Matzanke, B. F., Drapal, N. M., Jacobi, A., and Bock, A. (2004) The complex between hydrogenase-maturation proteins HypC and HypD is an intermediate in the supply of cyanide to the active site iron of [NiFe]-hydrogenases. *J. Mol. Biol.* **344,** 155–167
75. Volbeda, A., Charon, M. H., Piras, C., Hatchikian, E. C., Frey, M., and Fontecilla-Camps, J. C. (1995) Crystal structure of the nickel-iron hydrogenase from *Desulfovibrio gigas. Nature* **373,** 580–587
76. Manyani, H., Rey, L., Palacios, J. M., Imperial, J., and Ruiz-Argueso, T. (2005) Gene products of the *hupGHIJ* operon are involved in maturation of the iron-sulfur subunit of the [NiFe] hydrogenase from *Rhizobium leguminosarum* bv. viciae. *J. Bacteriol.* **187,** 7018–7026
77. Huang, H., Jedynak, B. M., and Bader, J. S. (2007) Where have all the interactions gone? Estimating the coverage of two-hybrid protein interaction maps. *PLoS Comput. Biol.* **3,** e214
78. von Mering, C., Jensen, L. J., Kuhn, M., Chaffron, S., Doerks, T., Kruger, B., Snel, B., and Bork, P. (2007) STRING 7—recent developments in the integration and prediction of protein interactions. *Nucleic Acids Res.* **35,** D358–D362